

TriangleMix: A Lossless and Efficient Attention Pattern for Long Context Prefilling

Zhiyuan He¹, Yike Zhang^{2*}, Chengruidong Zhang¹, Huiqiang Jiang¹,
Yuqing Yang¹, Lili Qiu¹

¹Microsoft Research, ²Tsinghua University
zhiyuhe@microsoft.com

Abstract

Large Language Models (LLMs) rely on attention mechanisms whose time complexity grows quadratically with input sequence length, creating significant computational bottlenecks during the prefilling stage. Existing static sparse attention methods typically degrade accuracy, while dynamic sparsity methods introduce additional computational overhead due to runtime sparse index estimation. To address these limitations, we propose TriangleMix, a novel training-free static attention pattern. TriangleMix employs dense attention in shallow layers and switches to a triangle-shaped sparse pattern in deeper layers. Extensive experiments demonstrate that TriangleMix reduces attention overhead by $3.7\times$ to $15.3\times$ in deep layers, and decreases overall Time-to-First-Token (TTFT) by 12% to 32% for sequence lengths ranging from 32K to 128K, without sacrificing model accuracy. Moreover, TriangleMix can be seamlessly integrated with dynamic sparsity methods to achieve further speedup, e.g. accelerating MInference by 19% at 128K, highlighting its potential to enhance LLM inference efficiency. [†]

1 Introduction

Large Language Models (LLMs) are capable of processing input sequences of varying lengths (Grattafiori et al., 2024; Achiam et al., 2023; Yang et al., 2024), a crucial ability that supports diverse downstream tasks, such as question answering (Bai et al., 2023), long-form document understanding (Zhao et al., 2024), and code generation (Jiang et al., 2024b). However, due to the quadratic complexity of attention mechanisms, the time-to-first-token (TTFT) significantly increases as the input context length grows. As prior research has demonstrated, attention computation has become a critical

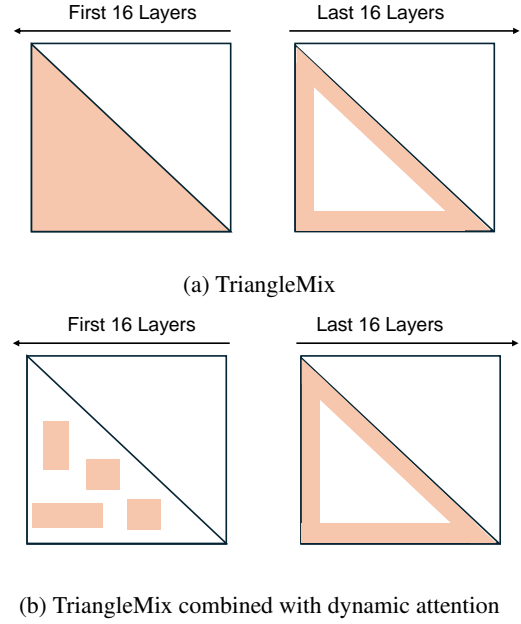


Figure 1: TriangleMix on Llama-3.1-8B-Instruct.

bottleneck in the prefilling stage of LLMs (Jiang et al., 2024a; Lai et al., 2025).

To address this bottleneck and accelerate the prefilling stage, researchers have proposed both static and dynamic sparse attention methods. Static sparse attention methods, such as StreamingLLM (Xiao et al., 2023), reduce computational complexity from $O(N^2)$ to $O(N)$ but suffer notable performance degradation on tasks with long contexts (Li et al., 2024a). On the other hand, dynamic sparsity approaches, such as MInference (Jiang et al., 2024a) and FlexPrefill (Lai et al., 2025), aim to maintain near-full performance by dynamically computing sparse attention indices during inference.

Dynamic sparsity methods are effective for handling extremely long contexts (e.g., beyond 128K tokens). However, they incur additional overhead due to the runtime estimation of sparse block indices. While this overhead is negligible at very long

*Work during internship at Microsoft.

[†]Implementation at <https://aka.ms/TriangleMix>

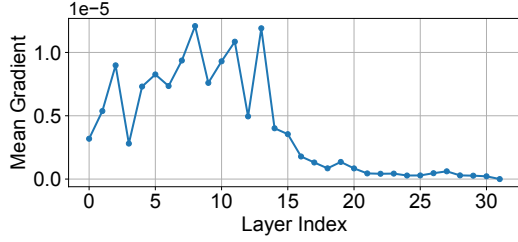


Figure 2: The average gradient $\text{Grad}(\mathbf{M}, l)$ of the Middle Q-K sections, measured on Llama-3.1-8B-Instruct, shows a significant decline in deeper layers. This suggests that *the Middle Q-K components in deeper layers contribute minimally* and might potentially be skipped to improve efficiency.

sequence lengths, it becomes non-trivial for moderately long contexts ranging from 32K to 128K tokens. We measured the average attention kernel time per layer on Llama-3.1-8B-Instruct, and the results (Table 1) show that MInference can be 2× slower than dense attention at 32K, and offers only limited speedup at 64K. Similarly, FlexPrefill delivers a modest 1.4× speedup at 32K.

In this work, we aim to develop a static attention pattern that effectively accelerates the pre-filling stage across various context lengths. To achieve this goal, we propose a novel gradient-based method to identify the crucial sections within attention maps. Our analysis demonstrates that the middle Q-K section (Figure 2 and 3) of the attention map can be safely omitted in deeper layers without incurring performance loss. Motivated by this insight, we introduce *TriangleMix*, a lossless and efficient static attention pattern for accelerating long-context LLMs. As depicted in Figure 1, TriangleMix applies standard dense attention in shallow layers, and switches to a triangle-shaped sparse attention pattern in deeper layers. TriangleMix offers four major advantages:

- It is training-free, enabling direct integration with state-of-the-art pretrained LLMs.
- It achieves nearly lossless accuracy, preserving the full capabilities of the underlying models.
- Its static triangle-shaped sparsity eliminates the need for dynamic block index estimation and reduces the computational complexity from $O(N^2)$ to $O(N)$.
- It is complementary to dynamic attention approaches. Replacing dynamic attention in deep layers with the static Triangle attention further enhances acceleration, compared with dynamic sparse attention alone.

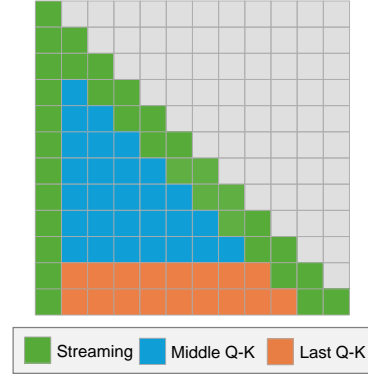


Figure 3: Three attention sections.

Method	32K	64K	128K
Dense	44	179	750
MInference	94	152	229
FlexPrefill ($\gamma = 0.95$)	32	71	220

Table 1: Averaged attention kernel time in milliseconds for one layer on Llama-3.1-8B-Instruct.

We conduct extensive experiments on three long-context LLMs, including Llama-3.1-8B-Instruct (Grattafiori et al., 2024), Llama-3-8B-Instruct-262K (GradientAI, 2024), and Qwen2.5-7B-Instruct (Yang et al., 2024), using all tasks from the RULER and LongBench benchmarks (Hsieh et al., 2024; Bai et al., 2023). The results demonstrate that TriangleMix maintains the same accuracy as full attention. For Llama-3.1-8B-Instruct, TriangleMix decreases overall TTFT by 12% to 32% across context lengths ranging from 32K to 128K. Moreover, it can be seamlessly combined with dynamic sparsity methods without degrading performance. For example, integrating TriangleMix with MInference decreases TTFT by 19% at 128K context length for Llama-3.1-8B-Instruct.

2 Methodology

2.1 Sparse Attention

The prefilling stage of Transformer attention can be formulated as:

$$\mathbf{A} = \text{Softmax}\left(\frac{1}{\sqrt{d}}\mathbf{Q}\mathbf{K}^T - c(1 - \mathbf{M})\right)$$

where $\mathbf{Q}, \mathbf{K}, \mathbf{V}$ are matrices of shape (N, d) , and \mathbf{M} is a causal mask matrix of shape (N, N) , with entries $M_{i,j} \in \{0, 1\}$. Here, N represents the number of input tokens, and c is a large positive constant to ensure attention scores masked by

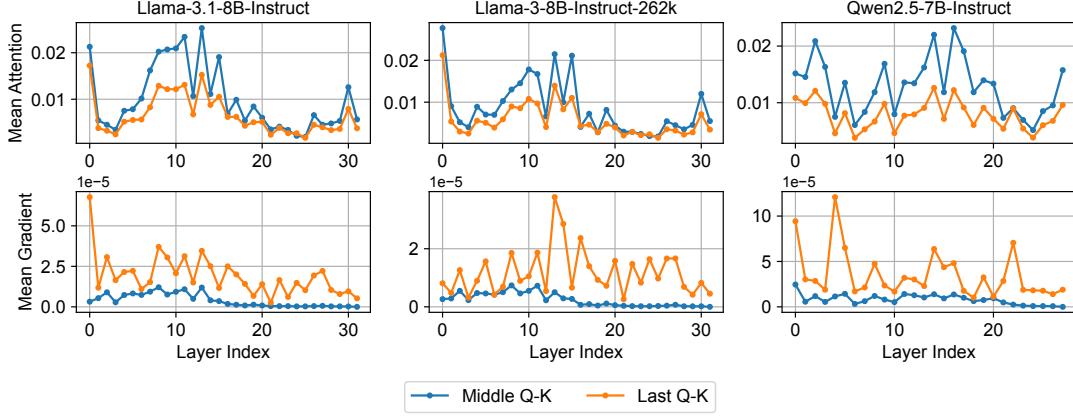


Figure 4: First row: Average attention score $\text{Att}(\mathbf{M}, l)$ for the Middle and Last Q-K sections; Second row: average gradient $\text{Grad}(\mathbf{M}, l)$ for the Middle and Last Q-K sections.

$M_{i,j} = 0$ become effectively zero after the softmax operation.

To accelerate computing, sparse attention aims to find a sparse mask matrix M' to compute the attention output:

$$\mathbf{A}' = \text{Softmax}\left(\frac{1}{\sqrt{d}}\mathbf{Q}\mathbf{K}^T - c(1 - M')\right)$$

where $|\mathbf{A} - \mathbf{A}'|$ is expected to be sufficiently small to preserve the original model performance.

Existing sparse attention methods fall into two categories: static sparsity and dynamic sparsity. In static sparsity, the sparse mask M' is fixed and does not depend on the input. For example, StreamingLLM shows that most attention scores accumulate on the first few sink tokens and nearby tokens in a sliding window (Xiao et al., 2023). This leads to the following streaming pattern:

$$M_{i,j}^{\text{streaming}} = \begin{cases} 1, & i \geq j, j \leq si \\ 1, & i \geq j, i - j \leq sl \\ 0, & \text{otherwise} \end{cases}$$

where si is the number of sink tokens and sl is the sliding window size. This pattern, also called "A-shape" in previous works (Jiang et al., 2024a), is very efficient with only $O(N)$ complexity. However, it causes significant performance drops for long-context LLMs (Li et al., 2024a). In contrast, dynamic sparsity methods, such as MInference (Jiang et al., 2024a) and FlexPrefill (Lai et al., 2025), estimate M' at inference time based on the input through an observation window or the pooling vector of \mathbf{Q} and \mathbf{K} .

Dynamic sparsity generally provides better accuracy and acceleration for extremely long contexts

(e.g., contexts exceeding 128K tokens). However, for moderately long contexts, the online estimation introduces additional time overhead. Specifically, as demonstrated in Table 1, MInference is slower than dense attention or offers small acceleration for contexts below 64K, while FlexPrefill achieves only modest improvements (approximately 1.4x speedup for 32K context).

2.2 Attention Sections

In this paper, we aim to design a static sparse attention mask that is both efficient and effective. Although a large fraction of attention scores falls into the streaming pattern, a significant performance gap still remains between streaming sparse attention and full dense attention. This leads us to the following question:

Beyond the streaming pattern, what other parts of the attention are crucial for maintaining the end-to-end performance of long-context LLMs?

To answer this, we divide the full attention matrix into three distinct sections as illustrated in Figure 3:

- Streaming section: includes attention sink and the sliding window;
- Last Q-K section: covers interactions between the last part of \mathbf{Q} and \mathbf{K} , excluding the Streaming section;
- Middle Q-K section: consists of the remaining interactions between the middle parts of \mathbf{Q} and \mathbf{K} .

We define the Last Q-K mask as:

$$M_{i,j}^{\text{last}} = \begin{cases} 1, & i \geq j, N - i < \text{last}, \\ & j > si, i - j > sl \\ 0, & \text{otherwise} \end{cases}$$

where $\text{last} \geq 1$ specifies the number of rows corresponding to the last section.

Similarly, the Middle Q-K mask is defined as:

$$M_{i,j}^{\text{middle}} = \begin{cases} 1, & i \geq j, N - i \geq \text{last}, \\ & j > si, i - j > sl \\ 0, & \text{otherwise} \end{cases}$$

2.3 Probing Attention Importance

Firstly, we inspect the average attention scores within the two sections defined by masks M^{middle} and M^{last} . We observe that these average attention scores are quite similar, although both are notably lower than the average score observed in the streaming section $M^{\text{streaming}}$. To achieve a more precise measurement of the relative importance of these sections, we introduce a novel gradient-based probing technique.

Specifically, given an input X_{input} containing N tokens fed into a language model, we define a probing variable $\theta \in \mathbb{R}^{L \times N \times N}$, where $\theta_{\ell,i,j} = 1$ for all layers ℓ and token indices i, j . Here, L represents the total number of layers in the model. For simplicity of notation, we omit the attention head dimension here, but our proposed method generalizes naturally to both Multi-head Attention (Vaswani et al., 2017) and Grouped Query Attention (Ainslie et al., 2023).

In layer l , the attention scores is calculated as:

$$A_{\theta} = \theta_l \odot \text{Softmax} \left(\frac{1}{\sqrt{d}} QK^T - c(1 - M) \right)$$

where \odot denotes element-wise multiplication. Since all elements of θ are initially set to 1, this operation does not alter the attention scores.

The model then outputs a logit prediction Y_{θ} for the next token, represented as a vector $Y_{\theta} = [y_1, y_2, \dots, y_{\text{vocab}}]$. Our focus is on a specific logit y_{gt} , associated with the correct label or ground truth token. For instance, the correct answer in a multiple-choice scenario or the initial token of the target sequence in a needle-in-a-haystack task.

We are particularly interested in the partial derivative $\frac{\partial y_{\text{gt}}}{\partial \theta_{l,i,j}}$, which measures the sensitivity of the model’s output to changes in attention scores.

We quantify the importance of a specific attention section by computing the mean of the derivative values within that section. Formally, we define the gradient-based importance as:

$$\text{Grad}(M, l) = \frac{\sum_{M_{i,j}=1} \frac{\partial y_{\text{gt}}}{\partial \theta_{l,i,j}}}{\sum_{M_{i,j}=1} M_{i,j}}$$

where M denotes the binary mask representing the targeted attention section, and $\text{Grad}(M, l)$ indicates the average sensitivity of y_{gt} to changes within this section at layer l .

For comparison, we also define the average attention score of the section as:

$$\text{Att}(M, l) = \frac{\sum_{M_{i,j}=1} A_{l,i,j}}{\sum_{M_{i,j}=1} M_{i,j}}$$

where $A_{l,i,j}$ represents the attention score at positions (i, j) in layer l .

Empirically, we leverage a key-value retrieval task to analyze the importance of different sections of attention. The language model is tasked with retrieve the corresponding value, starting from its first generated token. y_{gt} is set to be the first token of the correct value. The full task prompt is provided in Appendix A.1.

We calculate $\text{Grad}(M, l)$ and $\text{Att}(M, l)$ for both the middle Q-K section (M^{middle}) and the last Q-K section (M^{last}) across 100 randomly generated samples. The hyperparameters are set as follows: the number of sink tokens (si) is 64, the sliding window size (sl) is 128, and the length of the last attention section (last) is also set to 128. Each input sequence consists of approximately 2,000 tokens. Finally, we visualize the results for $\text{Grad}(M, l)$ and $\text{Att}(M, l)$ in Figure 4. For clarity, attention scores and gradient values are both summed across all heads within each layer.

2.4 TriangleMix

From Figure 4, we observe that both the Middle Q-K and Last Q-K sections have low average attention scores, with the Middle Q-K section slightly higher across all layers. However, when examining the gradient values, we find that the derivatives in the Last Q-K section are significantly larger than those in the Middle Q-K section. This indicates that the model output is more sensitive to changes in the attention scores of the Last Q-K section compared to the Middle Q-K section.

Besides, for the last layer, we observe that we always have $\text{Grad}(M, l) = 0$. This phenomenon

Methods	Average	2Wiki	GovRep	Hotpot	LCC	MNews	MF-en	PsgCnt	PsgRtr	Qasper	Rbench	Samsun	TREC	TrvQA
<i>Llama-3.1-8B-Instruct</i>	54.8	48.1	34.4	61.6	66.6	25.6	56.9	16.8	99.7	44.9	52.7	42.6	71.0	91.6
Streaming	34.7	17.4	32.2	19.8	65.6	24.6	25.6	5.7	11.8	23.3	54.1	40.6	52.7	77.3
Triangle	47.0	40.6	33.2	52.3	63.6	24.6	53.5	7.9	42.0	46.3	46.5	43.0	67.0	90.1
StreamingMix	48.9	36.4	34.3	39.4	64.9	25.8	42.3	18.4	98.3	42.4	53.6	42.6	51.0	86.8
DuoAttention	54.5	44.6	34.1	59.1	68.0	25.3	55.0	15.7	99.7	43.9	58.8	42.7	71.3	91.0
TriangleMix	54.5	47.8	34.3	61.5	67.0	25.8	56.5	16.8	98.3	44.8	51.9	42.2	69.7	92.2
<i>Llama-3-8B-Instruct-262k</i>	44.2	21.0	34.3	26.4	46.1	26.3	50.2	4.7	95.0	30.5	43.3	41.1	68.3	86.8
Streaming	30.8	16.8	34.3	18.5	41.8	25.3	39.6	0.3	10.0	23.4	36.5	38.6	49.0	66.0
Triangle	36.2	17.1	34.1	21.2	35.5	25.3	50.0	5.0	32.0	28.9	32.4	40.5	63.0	85.9
StreamingMix	39.9	18.5	34.4	19.8	42.3	25.9	47.4	5.3	85.0	30.0	38.3	40.1	48.3	83.3
DuoAttention	42.6	19.2	34.6	25.1	44.4	26.1	51.8	2.3	87.7	29.6	41.1	40.4	65.7	85.9
TriangleMix	43.4	20.7	34.5	25.7	47.3	26.1	51.1	4.7	85.3	30.7	43.6	40.9	66.7	87.0
<i>Qwen2.5-7B-Instruct</i>	46.8	24.5	30.7	32.2	62.2	22.3	41.3	13.1	99.3	24.4	60.7	42.5	67.0	88.7
Streaming	28.3	10.1	31.3	9.5	61.7	21.5	20.7	6.5	8.2	11.4	44.8	40.2	51.7	49.9
Triangle	36.9	17.4	27.5	24.0	48.5	17.9	38.5	5.6	43.9	22.3	39.6	41.2	65.0	88.1
StreamingMix	45.2	24.4	31.9	38.5	68.2	22.5	43.5	10.7	93.0	24.8	60.9	42.0	43.7	83.1
TriangleMix	46.2	25.7	30.4	32.2	61.1	22.3	41.7	12.9	89.0	24.4	61.4	42.1	68.7	88.9

Table 2: Comparison with static sparsity methods on Longbench. TriangleMix is our proposed method. StreamingMix is a hybrid baseline that uses dense attention in shallow layers but replaces Triangle attention with a streaming pattern in deeper layers. The number of dense layers matches that of TriangleMix.

is expected due to the specific structure of the attention mechanism. In the last layer, the logit corresponding to the first predicted token is computed solely based on the last query vector and the entire key matrix K^T . Formally, this corresponds to computing only the last row of the attention map, represented as $\text{Softmax}(Q_{\text{last}} K^T)$. Since the gradient measure $\text{Grad}(M, l)$ is defined based on the derivative of the ground truth output logit with respect to parameters associated with the attention sections defined by the mask, and because the first output token logit does not depend on the Middle Q-K sections in the last layer (which involve query vectors from other positions), the resulting gradient naturally becomes zero.

During the training phase, this observation does not apply. The training loss is typically computed using all output logits across the entire input sequence, which requires calculating the full attention matrix in the last layer. However, during inference, since our primary interest lies only in the prediction, we can optimize the computation in the final layer by restricting attention calculation to $\text{Softmax}(\frac{1}{\sqrt{d}} Q_{\text{last}} K^T)$.

Moreover, we observe that the gradient values for the Middle Q-K sections follow a consistent trend across all models: they remain moderate in the shallow layers but drop sharply in deeper layers. As shown in Figure 2, this pattern is evident. For Llama-3.1-8B-Instruct and Llama-3-8B-Instruct-262K, the decline occurs between layers 10 and 20, while for Qwen2.5-7B-Instruct, it starts after layer 20.

This suggests that the attention from the Middle Q-K sections in deep layers contribute less to the output logits. Notably, the number of elements in the Middle Q-K sections scales quadratically with the input token length N , whereas the elements in the Streaming and Last Q-K sections grow only linearly with N . Therefore, if the computation of the Middle Q-K sections is skipped in deep layers, the time complexity of attention can be reduced from $O(N^2)$ to $O(N)$. And we assume such skipping will not cause significant loss in output quality.

Based on these observations, we propose **TriangleMix**, an effective and efficient static attention pattern designed for long-context LLMs. We denote the starting layer of Triangle attention as $L_{\text{tri_start}}$. For layer $l \leq L_{\text{tri_start}}$, we apply standard dense attention:

$$\text{Softmax}\left(\frac{1}{\sqrt{d}} Q K^T - c(1 - M)\right)$$

where M is the standard causal attention mask.

In layer $l > L_{\text{tri_start}}$, we skip the Middle Q-K sections and apply a Triangle-shape attention pattern:

$$\text{Softmax}\left(\frac{1}{\sqrt{d}} Q K^T - c(1 - (M - M^{\text{middle}}))\right)$$

where M^{middle} represents the mask corresponding to the Middle Q-K sections.

Thus, in deep layers, the attention complexity becomes $O(N)$, and there is no need for dynamic

estimation of the attention mask, making the computation highly efficient. Furthermore, we can optionally adopt dynamic sparse attention in shallow layers to further accelerate computation, while keeping the static Triangle pattern in deep layers.

We acknowledge that the Triangle-shape attention pattern was first introduced in Scbench (Li et al., 2024a). However, Scbench applies the Triangle-shape attention uniformly across all layers, leading to notable performance degradation. In contrast, by using a gradient-based probing method, we find that the Middle Q-K sections remain important in shallow layers. Therefore, by combining dense (or dynamic sparse) attention in shallow layers and Triangle-shape attention in deep layers, TriangleMix preserves model performance while achieving significant efficiency gains.

3 Evaluations

3.1 Settings

LLMs. We evaluate our method on the following long-context language models. (1) *Llama-3.1-8B-Instruct*, a state-of-the-art model from Meta with a context window of up to 128K tokens (Grattafiori et al., 2024). (2) *Llama-3-8B-Instruct-262K*, a fine-tuned variant from Llama-3-8B-Instruct that supports up to 262K tokens (GradientAI, 2024). (3) *Qwen2.5-7B-Instruct*, a model from Alibaba with a maximum context window of 128K (Yang et al., 2024).

Static Sparsity Baselines. We compare our method with four static sparsity baselines. The first is the Streaming pattern (Xiao et al., 2023), applied to all layers with $si = 8$ and $sl = 512$. The second is Triangle Attention applied to all layers, using $si = 8$, $sl = 512$, and $last = 128$. The third is a hybrid baseline StreamingMix, where dense attention is used for layers $l \leq L_{tri_start}$, and streaming attention is used for deeper layers.

We also compare against DuoAttention, which learns a separate sparsity pattern for each attention head (Xiao et al., 2024). DuoAttention provides a trained pattern for Llama-3.1-8B-Instruct; we train a sparsity pattern for Llama-3-8B-Instruct-262K using the authors’ script. However, for Qwen2.5-7B-Instruct, the training does not converge, so its result is omitted. At the prefilling stage, half of the heads follow the streaming pattern, while the other half use dense attention.

Dynamic Sparsity Baselines. We compare with two dynamic sparsity methods: MInference (Jiang

et al., 2024a) and FlexPrefill (Lai et al., 2025). We apply default sparsity settings of all LLMs from MInference. For FlexPrefill, we test its hyperparameter $\gamma = 0.90$ and $\gamma = 0.95$. Additionally, our method can be combined with dynamic sparsity attention: Dynamic sparsity (MInference or FlexPrefill) is applied for layers $l \leq L_{tri_start}$, while Triangle Attention is used for deeper layers. This combination reduces runtime overhead because Triangle Attention avoids runtime mask estimation in dynamic sparse attention. We use “Ours + MInference” and “Ours + FlexPrefill” to denote the corresponding combined versions.

Hyperparameters. The hyperparameter L_{tri_start} determines the layer from which the Triangle Attention pattern is applied. For layers $l \leq L_{tri_start}$, we use dense attention or dynamic sparsity methods. For layers $l > L_{tri_start}$, we switch to the static Triangle Attention. Based on the observations in Figure 4, we set $L_{tri_start} = 16$ for Llama-3.1-8B-Instruct and Llama-3-8B-Instruct-262K, and $L_{tri_start} = 20$ for Qwen2.5-7B-Instruct. For the Triangle mask, we use: sink tokens $si = 8$, sliding window size $sl = 512$, and last window size $last = 128$, which is the same with the sparse sparsity baselines.

Benchmarks. We evaluate on two benchmarks: (1) RULER: A synthetic long-context benchmark including tasks like hay-in-the-stack, KV retrieval, variable tracking, and QA. We evaluate at input lengths of 4K, 8K, 16K, 32K, 64K, and 128K, with 100 samples per task-length pair (Hsieh et al., 2024). (2) LongBench: A realistic long-context benchmark with tasks such as single-doc and multi-doc QA, few-shot learning, code generation, retrieval, summarization, and counting (Bai et al., 2023). We evaluate all English tasks.

Specifically, Qwen2.5-7B-Instruct adopts Yarn scaling to improve its long context ability for input length larger than 32K (Peng et al., 2023). We report the performance of the origin Qwen2.5-7B-Instruct model for RULER length $< 32K$, and the Yarn-scaled model for RULER length 32K, 64K and 128K. For LongBench, we only evaluate the origin Qwen2.5-7B-Instruct model for simplicity.

3.2 Effectiveness of TriangleMix

Comparison with Static Sparsity. Table 3 and Table 2 present the evaluation results of TriangleMix and various static sparsity baselines. TriangleMix consistently outperforms all static baselines and remains nearly lossless performance across all input

Methods	4K	8K	16K	32K	64K	128K	Avg.
<i>Llama-3.1</i>	96.6	95.3	94.8	91.3	86.3	78.1	90.4
Streaming	64.1	55.4	40.5	28.9	26.7	3.3	36.5
Triangle	88.8	88.3	82.8	72.6	65.0	39.0	72.7
StreamingMix	94.3	91.8	90.2	86.2	79.2	71.9	85.6
DuoAttention	95.7	93.1	88.4	84.3	82.5	64.0	84.7
TriangleMix	96.3	95.1	94.7	91.3	86.3	77.5	90.2
<i>Llama-3-262k</i>	93.4	90.3	88.8	85.1	82.2	79.4	86.5
Streaming	49.4	38.7	33.4	30.2	26.5	21.7	33.3
Triangle	88.1	84.7	80.6	71.0	65.0	55.4	74.1
StreamingMix	87.3	83.2	80.8	79.9	77.6	70.8	79.9
DuoAttention	92.8	91.9	89.0	85.0	81.1	76.1	86.0
TriangleMix	93.5	91.0	88.1	85.0	82.4	79.6	86.6
<i>Qwen2.5</i>	95.8	93.6	92.6	84.5	81.9	67.4	86.0
Streaming	55.6	47.8	35.9	30.6	28.1	21.0	36.5
Triangle	88.4	81.9	74.0	58.3	51.0	14.6	61.4
StreamingMix	93.3	90.4	89.4	81.7	76.4	63.6	82.5
TriangleMix	95.5	93.7	92.3	83.9	80.2	66.4	85.3

Table 3: Comparison with static sparsity methods on RULER. Llama-3.1, Llama-3-262K, Qwen2.5 are abbreviations for Llama-3.1-8B-Instruct, Llama-3-8B-262K, and Qwen2.5-8B-Instruct. The same applies to Table 4.

lengths. In contrast, other static methods usually suffer noticeable performance degradation. DuoAttention performs comparably to TriangleMix on LongBench using Llama-3.1-8B-Instruct. However, its performance is worse than TriangleMix on RULER, especially deteriorates at longer lengths (e.g., 64K and 128K). Furthermore, DuoAttention requires a separate training phase to learn head-wise sparsity patterns, which introduces additional computational overhead and may fail to converge on models such as Qwen-2.5-7B-Instruct.

On the LongBench benchmark, we observe that the full Triangle pattern performs poorly on PassageRetrieval tasks, while the StreamingMix pattern underperforms on the in-context learning task (TREC). These findings suggest that attention over the Middle Q-K section in shallow layers is crucial for retrieval tasks, while attention over the Last Q-K section in deeper layers plays a key role in supporting in-context learning.

Comparison with Dynamic Sparsity. Table 4 and Table 8 report results comparing TriangleMix with dynamic sparsity methods, as well as their combinations. FlexPrefill when $\gamma = 0.90$ usually leads to performance degradation, and MInference generally outperforms it. While the performance of MInference and FlexPrefill with $\gamma = 0.95$ is similar on the RULER benchmark, MInference still achieves better results on LongBench. When combined with either MInference or FlexPrefill, TriangleMix al-

ways fully retains the original performance of the dynamic sparsity methods. Moreover, combining TriangleMix with FlexPrefill even yields slight performance gains, particularly with Llama-3.1-8B-Instruct and Qwen-2.5-7B-Instruct.

Overall, TriangleMix preserves the full accuracy of dense attention across tasks while significantly reducing time complexity from $O(N^2)$ to $O(N)$ for layers $l > L_{\text{tri_start}}$.

Methods	4K	8K	16K	32K	64K	128K	Avg.
<i>Llama-3.1</i>	96.6	95.3	94.8	91.3	86.3	78.1	90.4
MInference	96.3	95.1	95.0	90.5	86.8	75.0	89.8
Ours + MInfer	96.2	95.0	94.5	90.8	87.2	75.8	89.9
FlexPrefill (0.90)	90.1	89.7	89.4	89.1	82.0	74.1	85.7
Ours + FP (0.90)	90.1	90.2	89.9	88.9	83.2	73.6	86.0
FlexPrefill (0.95)	95.0	94.7	94.5	92.8	86.5	75.9	89.9
Ours + FP (0.95)	95.2	95.0	94.7	92.8	86.8	76.2	90.1
<i>Llama-3-262k</i>	93.4	90.3	88.8	85.1	82.2	79.4	86.5
MInference	93.4	90.7	88.8	85.1	82.6	80.1	86.8
Ours + MInfer	93.0	90.4	88.6	84.4	82.7	80.1	86.5
FlexPrefill (0.90)	82.4	80.0	80.7	76.2	74.5	69.1	77.1
Ours + FP (0.90)	83.0	79.3	80.1	75.9	75.0	68.8	77.0
FlexPrefill (0.95)	90.3	87.7	88.0	83.8	80.2	75.7	84.3
Ours + FP (0.95)	90.2	87.3	87.3	83.8	80.0	76.6	84.2
<i>Qwen2.5</i>	95.8	93.6	92.6	84.5	81.9	67.4	86.0
MInference	95.6	93.8	92.8	84.9	79.1	68.0	85.7
Ours + MInfer	95.4	93.6	92.5	84.1	77.4	67.4	85.1
FlexPrefill (0.90)	84.4	79.4	82.4	71.4	65.4	47.7	71.8
Ours + FP (0.90)	86.4	80.5	84.2	72.6	67.2	48.3	73.2
FlexPrefill (0.95)	91.1	89.7	88.5	75.4	72.5	51.2	78.1
Ours + FP (0.95)	92.5	90.9	89.8	76.6	72.4	50.1	78.7

Table 4: Comparison with dynamic sparsity methods on RULER.

3.3 Analysis of Start Layer

In this section, we investigate the choice of $L_{\text{tri_start}}$ for each LLM. We evaluate all models on the 64K length tasks in the RULER benchmark, sweeping $L_{\text{tri_start}}$ from 0 to the total number of layers with a step size of 2. As shown in Figure 5, Llama-3.1-8B-Instruct and Llama-3-8B-Instruct-262K exhibit similar patterns: setting $L_{\text{tri_start}} = 12$ retains 99.7% and 100.0% of their original performance, respectively. This indicates that 62.5% of the layers can adopt the $O(N)$ Triangle Attention without noticeable degradation. In contrast, Qwen-2.5-7B-Instruct requires a higher threshold: setting $L_{\text{tri_start}} = 20$ retains 97.9% of the performance, corresponding to a sparsity ratio of 28.6%.

3.4 Efficiency of TriangleMix

We implement Triangle Attention using Triton (Tillet et al., 2019), with further implemen-

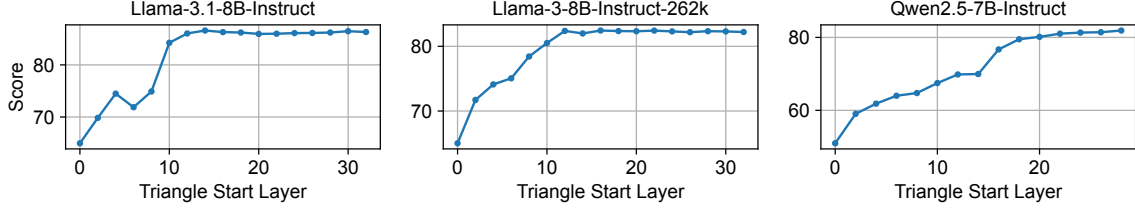


Figure 5: Average RULER score at 64K length for different $L_{\text{tri_start}}$ values.

Method	32K	64K	128K
Dense	44	179	750
MIInference	94 (0.5x)	152 (1.2x)	229 (3.3x)
FlexPrefill (0.95)	32 (1.4x)	71 (2.5x)	220 (3.4x)
FlexPrefill (0.90)	24 (1.8x)	52 (3.4x)	143 (5.2x)
Triangle	12 (3.7x)	24 (7.5x)	49 (15.3x)

Table 5: Attention kernel latency (ms) for one layer measured on Llama-3.1-8B-Instruct.

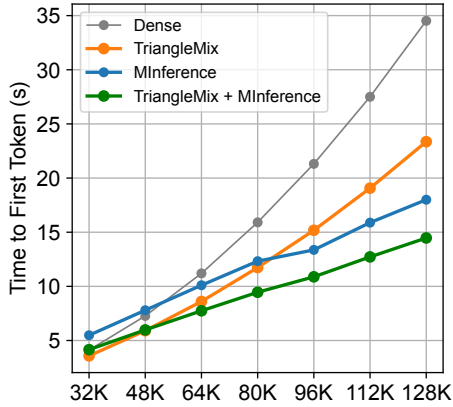


Figure 6: Time-to-first-token (TTFT) in seconds measured on Llama-3.1-8B-Instruct.

tation details provided in Appendix A.2. All experiments are conducted on a single NVIDIA A100 80GB GPU. Dense attention is implemented using FlashAttention (Kwon et al., 2023).

Attention Kernel Latency. We first benchmark the average attention kernel time per layer on Llama-3.1-8B-Instruct at sequence lengths of 32K, 64K, and 128K. As shown in Table 5, Triangle Attention significantly outperforms dense attention, achieving $3.7\times$ to $15.3\times$ speedup. The speedup mainly comes from Triangle Attention’s linear complexity ($O(N)$), which makes it much more efficient than $O(N^2)$ dense attention. Besides, unlike dynamic sparsity methods, it doesn’t require estimating attention block indices during runtime, which saves additional overhead.

End-to-End TTFT. We further measure time-to-first-token (TTFT) across sequence lengths of 32K, 48K, 64K, 96K, 112K, and 128K. Results for Llama-3.1-8B-Instruct are reported in Table 6. Tri-

angleMix applies dense attention in shallow layers and Triangle Attention in deeper layers, reducing TTFT by 12%–32%. It is also compatible with dynamic attention for enhanced performance. For example, integrating MIInference with TriangleMix reduces TTFT from 18.0s to 14.5s (a 19% decrease). Under the lossless setting, TriangleMix combined with FlexPrefill ($\gamma = 0.95$) achieves the fastest TTFT for 32K–80K sequences, while TriangleMix with MIInference is optimal for 96K–128K. We visualize the results of some selected methods in Figure 6.

4 Discussion

In this section, we discuss why Middle Q-K attention can be safely removed. Our hypothesis is that the observed phenomena arise from a *Train–Test Misalignment*. During training, the loss is applied uniformly to all positions in the input sequence. For example, if the input contains 2048 tokens, the model is also trained to predict token 1001 given tokens 1–1000. However, during inference, the primary goal is to predict tokens *after* the prompt (such as token 2049), making predictions of tokens *inside* the prompt (such as token 1001) largely irrelevant.

To validate this assumption, we conduct an experiment on Llama-3.1-8B-Instruct. We sample 100 Wikipedia articles and extract the first 2048 tokens of each. In the last 16 layers, we apply Triangle Attention, skipping attention for Q indices between 512 and 1024. We then measure changes of the average perplexity (PPL) relative to dense attention in two output spans.

The results in Table 7 show that skipping attention of Q index 512–1024 in deep layers noticeably increases perplexity when predicting tokens in the 1024–1152 range. For these positions, the skipped attention effectively becomes the Last Q-K attention necessary for predicting the next token. In contrast, for positions beyond 1920, the effect is minimal.

The Middle Q-K region is important primarily

Method	32K	48K	64K	80K	96K	112K	128K
Dense	4.1	7.3	11.2	15.9	21.3	27.5	34.5
MInference	5.5 (+34%)	7.8 (+7%)	10.1 (-10%)	12.3 (-23%)	13.4 (-37%)	15.9 (-42%)	18.0 (-48%)
FlexPrefill (0.95)	3.6 (-12%)	5.5 (-25%)	7.7 (-31%)	9.9 (-38%)	12.3 (-42%)	15.0 (-45%)	17.8 (-48%)
TriangleMix	3.6 (-12%)	5.9 (-19%)	8.6 (-23%)	11.7 (-26%)	15.2 (-29%)	19.1 (-31%)	23.4 (-32%)
Ours + MInference	4.2 (+2%)	6.0 (-18%)	7.7 (-31%)	9.5 (-40%)	10.9 (-49%)	12.7 (-54%)	14.5 (-58%)
Ours + FP (0.95)	3.4 (-17%)	5.2 (-29%)	7.2 (-36%)	9.2 (-42%)	11.3 (-47%)	13.6 (-51%)	16.1 (-53%)
FlexPrefill (0.90)	3.3 (-20%)	5.1 (-30%)	6.8 (-39%)	8.9 (-44%)	11.1 (-48%)	13.6 (-51%)	15.5 (-55%)
Ours + FP (0.90)	3.3 (-20%)	4.5 (-38%)	6.7 (-40%)	8.5 (-47%)	10.5 (-51%)	12.6 (-54%)	14.5 (-58%)

Table 6: Time-to-first-token (TTFT) in seconds measured on Llama-3.1-8B-Instruct. We separate FlexPrefill ($\gamma = 0.90$) as it generally leads to accuracy degradation, whereas the other settings do not.

Method	PPL (1024–1152)	PPL (1920–2048)
Dense	8.02	7.79
TriangleMix	8.34 (+0.32)	7.81 (+0.02)

Table 7: With 2048 input tokens, we measure perplexity on two output spans. Triangle attention is applied, skipping attention between Q indices 512–1024 in the last 16 layers. Experiments are on Llama-3.1-8B-Instruct.

for predicting tokens within the prompt, while for generation tasks focused on tokens after the prompt, the Middle Q-K in deeper layers is largely redundant. Although further theoretical work is needed, this observation suggests that selective sparsification of attention during inference can be done safely.

5 Related Works

Static Sparsity Attention. Early methods employ fixed sparse patterns, such as strided (Child et al., 2019), dilated (Ding et al., 2023), sliding window (Jiang et al., 2023), and mixed patterns (Beltagy et al., 2020), typically requiring training from scratch. DuoAttention (Xiao et al., 2024) introduces head-level static sparsity but needs additional offline training. Training-free approaches like Streaming (Xiao et al., 2023) and Triangle (Li et al., 2024a) attention often degrade accuracy for long contexts. In contrast, the proposed TriangleMix attention pattern significantly mitigates performance loss and is nearly lossless in accuracy.

Dynamic Sparsity Attention. Methods like MInference (Jiang et al., 2024a), FlexPrefill (Lai et al., 2025), and XAttention (Xu et al., 2025) dynamically determine attention masks online, maintaining high accuracy but incurring computational overhead for moderately long contexts. TriangleMix can enhance these dynamic approaches for further acceleration.

Long-context LLM Inference. FlashAttention

(Dao et al., 2022) speeds up attention by reducing memory access through fused operations. PageAttention (Kwon et al., 2023) improves decoding by managing KV cache allocation efficiently. KV cache optimizations techniques also include token-level eviction (SnapKV (Li et al., 2024b)) and query-aware cache selection (Quest (Tang et al., 2024)). TriangleMix is orthogonal to these approaches.

6 Conclusion

In this paper, we propose a hybrid attention pattern for long-context LLMs, where dense attention is used in shallow layers and Triangle attention is applied in deeper layers. This pattern is training-free and achieves nearly lossless accuracy. Our method achieves a 12% to 32% time-to-first-token reduction across 32K to 128K inputs. Moreover, it can be further accelerated when combined with dynamic sparsity attention.

Limitations

One limitation of our method is that the sparsity ratio is fixed within the pretrained model. We observe that Llama-3.1-8B-Instruct and Llama-3-8B-Instruct-262K exhibit higher inherent sparsity compared to Qwen2.5-7B-Instruct, which constrains the achievable acceleration on the latter. It may be possible to enhance the sparsity of models like Qwen2.5-7B-Instruct through a post-training optimization process, which we leave for future exploration.

References

Josh Achiam, Steven Adler, Sandhini Agarwal, Lama Ahmad, Ilge Akkaya, Florencia Leoni Aleman, Diogo Almeida, Janko Altschmidt, Sam Altman, Shyamal Anadkat, and 1 others. 2023. Gpt-4 technical report. *arXiv preprint arXiv:2303.08774*.

- Joshua Ainslie, James Lee-Thorp, Michiel De Jong, Yury Zemlyanskiy, Federico Lebrón, and Sumit Sanghai. 2023. Gqa: Training generalized multi-query transformer models from multi-head checkpoints. *arXiv preprint arXiv:2305.13245*.
- Yushi Bai, Xin Lv, Jiajie Zhang, Hongchang Lyu, Jiankai Tang, Zhidian Huang, Zhengxiao Du, Xiao Liu, Aohan Zeng, Lei Hou, and 1 others. 2023. Longbench: A bilingual, multitask benchmark for long context understanding. *arXiv preprint arXiv:2308.14508*.
- Iz Beltagy, Matthew E Peters, and Arman Cohan. 2020. Longformer: The long-document transformer. *arXiv preprint arXiv:2004.05150*.
- Rewon Child, Scott Gray, Alec Radford, and Ilya Sutskever. 2019. Generating long sequences with sparse transformers. *arXiv preprint arXiv:1904.10509*.
- Tri Dao, Dan Fu, Stefano Ermon, Atri Rudra, and Christopher Ré. 2022. Flashattention: Fast and memory-efficient exact attention with io-awareness. *Advances in neural information processing systems*, 35:16344–16359.
- Jiayu Ding, Shuming Ma, Li Dong, Xingxing Zhang, Shaohan Huang, Wenhui Wang, Nanning Zheng, and Furu Wei. 2023. Longnet: Scaling transformers to 1,000,000,000 tokens. *arXiv preprint arXiv:2307.02486*.
- GradientAI. 2024. [Llama-3 8b gradient instruct 262k](#).
- Aaron Grattafiori, Abhimanyu Dubey, Abhinav Jauhri, Abhinav Pandey, Abhishek Kadian, Ahmad Al-Dahle, Aiesha Letman, Akhil Mathur, Alan Schelten, Alex Vaughan, and 1 others. 2024. The llama 3 herd of models. *arXiv preprint arXiv:2407.21783*.
- Cheng-Ping Hsieh, Simeng Sun, Samuel Kriman, Shantanu Acharya, Dima Rekesht, Fei Jia, Yang Zhang, and Boris Ginsburg. 2024. Ruler: What’s the real context size of your long-context language models? *arXiv preprint arXiv:2404.06654*.
- Albert Q. Jiang, Alexandre Sablayrolles, Arthur Mensch, Chris Bamford, Devendra Singh Chaplot, Diego de las Casas, Florian Bressand, Gianna Lengyel, Guillaume Lample, Lucile Saulnier, L  lio Renard Lavaud, Marie-Anne Lachaux, Pierre Stock, Teven Le Scao, Thibaut Lavril, Thomas Wang, Timoth  e Lacroix, and William El Sayed. 2023. [Mistral 7b](#). *Preprint*, arXiv:2310.06825.
- Huiqiang Jiang, Yucheng Li, Chengruidong Zhang, Qianhui Wu, Xufang Luo, Surin Ahn, Zhenhua Han, Amir Abdi, Dongsheng Li, Chin-Yew Lin, and 1 others. 2024a. Minference 1.0: Accelerating pre-filling for long-context llms via dynamic sparse attention. *Advances in Neural Information Processing Systems*, 37:52481–52515.
- Juyong Jiang, Fan Wang, Jiasi Shen, Sungju Kim, and Sunghun Kim. 2024b. A survey on large language models for code generation. *arXiv preprint arXiv:2406.00515*.
- Woosuk Kwon, Zhuohan Li, Siyuan Zhuang, Ying Sheng, Lianmin Zheng, Cody Hao Yu, Joseph Gonzalez, Hao Zhang, and Ion Stoica. 2023. Efficient memory management for large language model serving with pagedattention. In *Proceedings of the 29th Symposium on Operating Systems Principles*, pages 611–626.
- Xunhao Lai, Jianqiao Lu, Yao Luo, Yiyuan Ma, and Xun Zhou. 2025. Flexprefill: A context-aware sparse attention mechanism for efficient long-sequence inference. *arXiv preprint arXiv:2502.20766*.
- Yucheng Li, Huiqiang Jiang, Qianhui Wu, Xufang Luo, Surin Ahn, Chengruidong Zhang, Amir H Abdi, Dongsheng Li, Jianfeng Gao, Yuqing Yang, and 1 others. 2024a. Scbench: A kv cache-centric analysis of long-context methods. *arXiv preprint arXiv:2412.10319*.
- Yuhong Li, Yingbing Huang, Bowen Yang, Bharat Venkitesh, Acyr Locatelli, Hanchen Ye, Tianle Cai, Patrick Lewis, and Deming Chen. 2024b. Snapkv: Llm knows what you are looking for before generation. *Advances in Neural Information Processing Systems*, 37:22947–22970.
- Bowen Peng, Jeffrey Quesnelle, Honglu Fan, and Enrico Shippole. 2023. Yarn: Efficient context window extension of large language models. *arXiv preprint arXiv:2309.00071*.
- Jiaming Tang, Yilong Zhao, Kan Zhu, Guangxuan Xiao, Baris Kasikci, and Song Han. 2024. Quest: Query-aware sparsity for efficient long-context llm inference. *arXiv preprint arXiv:2406.10774*.
- Philippe Tillet, Hsiang-Tsung Kung, and David Cox. 2019. Triton: an intermediate language and compiler for tiled neural network computations. In *Proceedings of the 3rd ACM SIGPLAN International Workshop on Machine Learning and Programming Languages*, pages 10–19.
- Ashish Vaswani, Noam Shazeer, Niki Parmar, Jakob Uszkoreit, Llion Jones, Aidan N Gomez, Łukasz Kaiser, and Illia Polosukhin. 2017. Attention is all you need. *Advances in neural information processing systems*, 30.
- Guangxuan Xiao, Jiaming Tang, Jingwei Zuo, Junxian Guo, Shang Yang, Haotian Tang, Yao Fu, and Song Han. 2024. Duoattention: Efficient long-context llm inference with retrieval and streaming heads. *arXiv preprint arXiv:2410.10819*.
- Guangxuan Xiao, Yuandong Tian, Beidi Chen, Song Han, and Mike Lewis. 2023. Efficient streaming language models with attention sinks. *arXiv preprint arXiv:2309.17453*.

- Ruyi Xu, Guangxuan Xiao, Haofeng Huang, Junxian Guo, and Song Han. 2025. Xattention: Block sparse attention with antidiagonal scoring. *arXiv preprint arXiv:2503.16428*.
- An Yang, Baosong Yang, Beichen Zhang, Binyuan Hui, Bo Zheng, Bowen Yu, Chengyuan Li, Dayiheng Liu, Fei Huang, Haoran Wei, and 1 others. 2024. Qwen2.5 technical report. *arXiv preprint arXiv:2412.15115*.
- Siyun Zhao, Yuqing Yang, Zilong Wang, Zhiyuan He, Luna K Qiu, and Lili Qiu. 2024. Retrieval augmented generation (rag) and beyond: A comprehensive survey on how to make your llms use external data more wisely. *arXiv preprint arXiv:2409.14924*.

A Appendix

A.1 Task to Probe Attention Importance

We use a key-value retrieval task to analyze the importance of different attention sections. The language model is prompted to retrieve the correct value, beginning from its first generated token. The prompt is as follows:

Prompt for Attention Importance Probing:

Extract the value corresponding to the specified key in the data below.

Data:

<key 1>: <value 1>

<key 2>: <value 2>

.....

<key n>: <value n>

Extract the value corresponding to this key:

key: {key i}

Please directly output the corresponding value without outputting anything else.
value:

We randomly generate pairs of keys and values using Version 4 UUID strings.

A.2 Implementation of Triangle Attention

We implement Triangle Attention using Triton (Tillet et al., 2019), with details provided in Algorithm 1. For each row index, we apply a different attention mechanism: if the row index is less than $N - N_{\text{last}}$, we apply Streaming Attention; otherwise, we apply chunked FlashAttention to increase GPU utilization. The outputs from both segments are then merged to produce the final result.

A.3 Additional Longbench Data

Table 8 compares our method with dynamic sparsity attention on Longbench. When combined with MInference, our method achieves similar performance to MInference alone. Integrating with Flex-Prefill yields a slight improvement over its original results.

Algorithm 1 Fused Triangle Attention

Input data: $Q, K, V \in \mathbb{R}^{N \times d_h}$

Input triangle shape: sink token number N_{sink} , sliding window size N_{window} , last rows number N_{last}

Input kernel block shape: B_M, B_N

Calculate best number of splits S for last row

Initialize $O \leftarrow (0)^{N \times d_h}$

Initialize output buffer $O_{\text{last}} \leftarrow (0)^{S N_{\text{last}} \times d_h}$

Initialize LSE buffer $l_{\text{last}} \leftarrow (-\inf)^{S N_{\text{last}}}$

Parallelized in GPU

for $i \leftarrow 1$ to $\lceil \frac{N - N_{\text{last}}}{B_M} \rceil + S \lceil \frac{N_{\text{last}}}{B_M} \rceil$ **do**

Initialize $O_{\text{chip}} \leftarrow (0)^{B_M \times d_h}$

Initialize $m \leftarrow (-\inf)^{B_N}$

Initialize $s \leftarrow (0)^{B_M}$

if $i \leq \lceil \frac{N - N_{\text{last}}}{B_M} \rceil$ **then**

Upper part: the same as streaming attention

Load $Q_{\text{chip}} \leftarrow Q^{i B_M : (i+1) B_M}$

Loop through sink tokens

for $j \leftarrow 1$ to $\lceil \frac{N_{\text{sink}}}{B_N} \rceil$ **do**

Load $K_{\text{chip}} \leftarrow K^{j B_N : (j+1) B_N}$

Load $V_{\text{chip}} \leftarrow V^{j B_N : (j+1) B_N}$

flash_attn($Q_{\text{chip}}, K_{\text{chip}}, V_{\text{chip}}, O_{\text{chip}}, m, s$)

end for

Loop through sliding window

for $j \leftarrow \lceil \frac{N - N_{\text{window}}}{B_N} \rceil$ to $\lceil \frac{N}{B_N} \rceil$ **do**

Load $K_{\text{chip}} \leftarrow K^{j B_N : (j+1) B_N} \in \mathbb{R}^{B \times d_h}$

Load $V_{\text{chip}} \leftarrow V^{j B_N : (j+1) B_N} \in \mathbb{R}^{B \times d_h}$

flash_attn($Q_{\text{chip}}, K_{\text{chip}}, V_{\text{chip}}, O_{\text{chip}}, m, s$)

end for

Write outputs

Save $O^{i B_M : (i+1) B_M} \leftarrow O_{\text{chip}}$

else

Last rows: split in to S chunks

Chunk index $c \leftarrow \lfloor (i - \lceil \frac{N - N_{\text{last}}}{B_M} \rceil) / \lceil \frac{N_{\text{last}}}{B_M} \rceil \rfloor$

Chunk offset $b \leftarrow (i - \lceil \frac{N - N_{\text{last}}}{B_M} \rceil) \bmod \lceil \frac{N_{\text{last}}}{B_M} \rceil$

Q index $i_Q \leftarrow \lceil \frac{N - N_{\text{last}}}{B_M} \rceil + b$

Load $Q_{\text{chip}} \leftarrow Q^{i_Q B_M : (i_Q + 1) B_M}$

for $j \leftarrow c \lceil \frac{N}{S B_N} \rceil$ to $(c + 1) \lceil \frac{N}{S B_N} \rceil$ **do**

Load $K_{\text{chip}} \leftarrow K^{j B_N : (j+1) B_N}$

Load $V_{\text{chip}} \leftarrow V^{j B_N : (j+1) B_N}$

flash_attn($Q_{\text{chip}}, K_{\text{chip}}, V_{\text{chip}}, O_{\text{chip}}, m, s$)

end for

Write outputs

Save $O_{\text{last}}^{(i - i_Q) B_M : (i - i_Q + 1) B_M} \leftarrow O_{\text{chip}}$

Save $l_{\text{last}}^{(i - i_Q) B_M : (i - i_Q + 1) B_M} \leftarrow \ln s + m$

end

end for

Merge last row output buffer

$O^{(N - N_{\text{last}}) : N} \leftarrow \text{merge_output}(O_{\text{last}}, l_{\text{last}})$

Methods	Average	2Wiki	GovRep	Hotpot	LCC	MNews	MF-en	PsgCnt	PsgRtr	Qasper	Rbench	Samsun	TREC	TrvQA
<i>Llama-3.1-8B-Instruct</i>	54.8	48.1	34.4	61.6	66.6	25.6	56.9	16.8	99.7	44.9	52.7	42.6	71.0	91.6
MIInference	54.9	48.1	34.5	61.4	67.0	25.9	57.0	17.5	99.7	44.7	52.5	42.6	71.3	91.9
Ours + MIInference	54.5	48.3	34.2	62.0	66.7	25.6	56.6	17.4	98.3	44.8	51.6	42.1	69.3	92.1
FlexPrefill; $\gamma = 0.90$	44.0	31.0	32.8	48.8	59.1	25.1	51.3	4.0	39.0	37.1	50.8	41.5	65.3	86.2
Ours + FlexPrefill; $\gamma = 0.90$	47.6	32.5	32.8	49.7	59.2	25.0	51.3	4.6	79.0	38.1	48.3	41.9	68.0	88.1
FlexPrefill; $\gamma = 0.95$	48.4	39.4	33.7	58.3	67.2	25.6	55.6	4.0	47.7	42.5	53.8	41.9	69.7	90.2
Ours + FlexPrefill; $\gamma = 0.95$	52.2	39.4	33.5	58.5	66.9	25.7	54.5	3.3	97.0	43.1	53.8	42.3	69.3	90.8
<i>Llama-3-8B-Instruct-262k</i>	44.2	21.0	34.3	26.4	46.1	26.3	50.2	4.7	95.0	30.5	43.3	41.1	68.3	86.8
MIInference	44.1	20.5	34.3	25.8	46.2	26.3	50.2	4.3	95.0	30.7	44.7	40.5	68.3	86.8
Ours + MIInference	43.4	20.6	34.4	26.4	47.2	26.2	51.1	4.3	85.3	30.3	43.6	40.9	66.7	86.9
FlexPrefill; $\gamma = 0.90$	33.6	16.8	32.7	23.0	46.8	25.6	45.6	2.3	8.0	23.2	41.4	36.8	61.0	73.3
Ours + FlexPrefill; $\gamma = 0.90$	33.9	16.5	32.8	22.4	48.5	25.7	46.1	3.3	12.3	23.0	39.5	37.1	59.7	73.8
FlexPrefill; $\gamma = 0.95$	35.0	17.7	33.0	25.1	36.8	26.1	49.1	3.3	13.7	28.3	36.2	39.1	65.0	81.7
Ours + FlexPrefill; $\gamma = 0.95$	36.0	18.3	33.2	25.1	36.9	26.2	49.6	6.7	24.0	28.3	35.6	38.9	64.3	80.4
<i>Qwen2.5-7B-Instruct</i>	46.8	24.5	30.7	32.2	62.2	22.3	41.3	13.1	99.3	24.4	60.7	42.5	67.0	88.7
MIInference	46.8	24.5	30.7	32.7	61.6	22.3	40.8	12.8	100.0	24.3	60.2	42.1	68.0	89.3
Ours + MIInference	46.2	24.3	31.0	33.4	61.3	22.2	41.7	11.6	90.3	23.8	61.4	42.1	68.0	89.1
FlexPrefill; $\gamma = 0.90$	37.3	17.5	29.3	27.6	64.0	21.8	39.0	7.0	28.7	15.1	51.4	39.3	64.7	79.3
Ours + FlexPrefill; $\gamma = 0.90$	38.7	18.2	29.4	28.8	64.1	21.7	38.7	7.3	38.3	15.8	52.4	39.1	68.0	80.7
FlexPrefill; $\gamma = 0.95$	40.8	20.2	29.7	33.9	66.8	21.8	40.4	4.0	48.7	17.1	54.8	40.5	67.3	85.5
Ours + FlexPrefill; $\gamma = 0.95$	41.5	19.8	30.2	33.9	65.0	21.8	40.3	4.9	56.0	16.8	55.2	40.2	69.7	85.8

Table 8: Comparison with dynamic sparsity methods on LongBench.